Prediction of spiralling in BTA deep-hole drilling – estimating the system's eigenfrequencies

G.Szepannek[1] N.Raabe[1] O.Webber[2] C.Weihs[1]

Februar 2006

[1]Fachbereich Statistik, Universität Dortmund, D-44221 Dortmund
[2]Institut für Spanende Fertigung, Universität Dortmund, D-44227 Dortmund

Abstract One serious problem in deep-hole drilling is the formation of a dynamic disturbance called spiralling which causes holes with several lobes. Since such lobes are a severe impairment of the bore hole quality the formation of spiralling has to be prevented. Gessesse et al. [2] explain spiralling by the coincidence of bending modes and multiples of the rotation frequency. They derive this from an elaborate finite elements model of the process.
In online measurements we detected slowly changing frequency patterns similar to those calculated by Gessesse et al. We therefore propose a method to estimate the parameters determining the change of frequencies over time from spectrogram data. This significantly simplifies the explanation of spiralling for practical applications compared to finite elements models which have to be correctly modified for each machine and tool assembly. It turns out that this simpler model achieves to explain the observed frequency patterns quite well.
We use this for estimating the variation of the frequencies as good as possible. This opens up the opportunity to prevent spiralling by e.g. changing the rotary frequency.

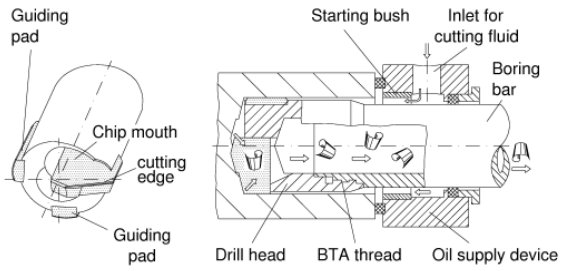

Figure 1: BTA deep hole drilling, working principle [10].

1 Introduction

The aim of the project is to analyze and model the BTA-deep-hole-drilling process. A longterm goal is to develop a tool for online-prediction of dynamic disturbances which in future may be used as a basis for intelligent control of the process.
Deep hole drilling methods are used for producing holes with a high length-to-diameter ratio, good surface finish and straightness. For drilling holes with a diameter of 20 mm and above, the BTA (Boring and Trepanning Association) deep hole machining principle is usually employed [10]. The working principle is illustrated in Fig. 1. Machining of bore holes with a high length to diameter ratio necessitates slender tool-boring bar assemblies. These components therefore have low dynamic stiffness properties which in turn can be the cause of dynamic disturbances such as *chatter vibration* and *spiralling*. Whereas chatter mainly leads to increased tool wear along with marks on the generally discarded bottom of the bore hole, spiralling causes a multi-lobe shaped deviation of the cross section of the hole from absolute roundness often constituting a significant impairment of the workpiece. The effects of these disturbances on the workpiece can be seen in Fig. 2.

As the deep hole drilling process is often used during the last production phases of expensive workpieces, process reliability is of prime importance. To achieve an optimal process design with the aim of reducing the risk of workpiece damage, a detailed analysis of the process dynamics is necessary. In this paper we focus on spiralling which can be observed to occur either

Figure 2: Radial chatter marks on the bottom of the bore hole (left) and effects of spiralling on the bore hole wall (right).

reproducibly at a certain drilling depth and fixed machining parameters or at random drilling depths [8]. Gessesse et al. [2] have modelled the process with finite elements and derived from this model and experimental observations that one reason for the reproducible occurrence of spiralling is the intersection of changing bending modes and uneven multiples of the rotational frequency of the tool or workpiece spindle. They have shown in some experiments that this actually was a good prediction of spiralling.
We observed the movement of the bending modes in online measurements of the bending moment of the boring bar and in measurements of the lateral acceleration of the boring bar.
A first approach to estimate the time course of the bending eigenfrequencies as it is proposed by Raabe et al. (2004) [6] is described in section 2. In this paper, we turn to the construction of a mechanical model of the boring bar. Such a model is hoped to more accurately calculate the course of the boring bar's eigenfrequencies over time. Unfortunately not all of the parameters for the model are known in advance. Therefore in this paper a method is presented to fit the model to the measured periodogram data. A first attempt to tackle this problem is developed by Raabe et al. (2005) [7]. The mechanical model is described in section 3. Then, section 4 introduces our criterion for parameter selection before some results are presented in section 5. The paper concludes with a summary given in section 7.

2 Estimation of the bending eigenfrequencies by polynomial regression on significant frequencies

In Raabe et al. (2004) [6] a two-step estimation process is proposed. First, a statistical test, developed by Theis (2004) [9] is used to identify the frequencies that are significantly dominating the process at any given point in time. These *relevant frequencies* are then grouped by cluster analytical methods into three clusters. The clusters are given by frequency bands, each of which is interpreted corresponding to some certain time course driven by one of the actual system's eigenfrequencies. This is illustrated in Figure 3, where different grey levels indicate different clusters. Finally, for each of the clusters, a polynomial regression is fitted to the data by minimizing the quadratic deviations of the estimated frequency (as a function of actual boring depth) to all 'relevant frequencies' of the cluster at this depth (see [6]).
Figure 3 illustrates the fit of the observed data by the procedure. A polynomial degree of 2 already allows a good fit for all clusters. As can be seen in the following sections, the amplitudes of the observed periodogram reflect the time course of the eigenfrequencies obtained by the mechanical model. In this paper we turn to estimation of the eigenfrequencies based on a mechanical model since their time course is more accurately represented by such a model.

3 Mechanical Model

To express the connection between the machine parameters and the time-variation of the bending eigenfrequencies (abbreviated BEF) from a mechanical point of view we propose a linear multi degree of freedom model (see Ewins et al. [1]) in the shape of a chain of coupled oscillators. For this purpose we let the structure of masses and stiffnesses in the model be determined by the BTA system's most important components (see Fig. 4), namely the tool-boring bar assembly, rigidly clamped at one end, in combination with the damper, the coolant supply device and the workpiece. The model is described below.

The illustration in Fig. 5 indicates that for our model we subdivide the bar into n segments – called elements – of equal length $l = L/n$ and mass

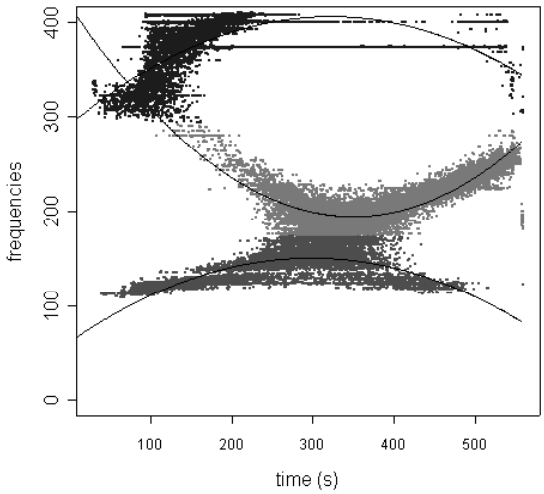

Figure 3: Cluster of relevant frequencies and polynomial fit of the periodogram data.

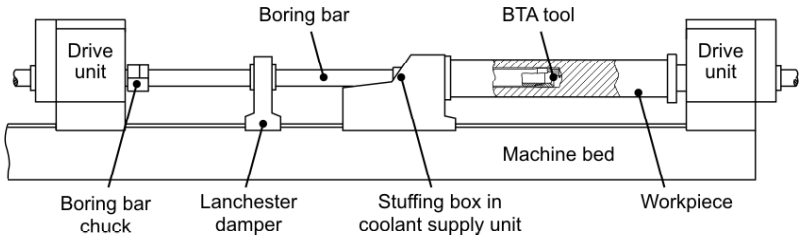

Figure 4: Components of the BTA boring bar.

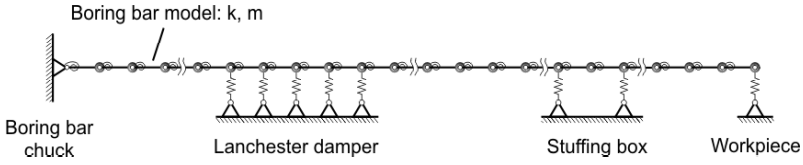

Figure 5: Components of the discretized analogous model.

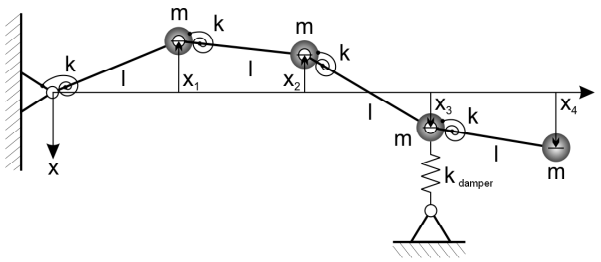

Figure 6: Example of the mechanical model with 4 degrees of freedom.

$m = M/n$, where L and M denote the corresponding values of the complete boring bar. The mass of each segment is modelled as a mass point located at the end of each segment. Each mass point is assumed to be connected to its neighbor via a massless rod in combination with a linear spiral spring of stiffness k. The leftmost mass point is connected in the same way to a rigid base. The number n is called the number of degrees of freedom. The details of the mechanical model are illustrated in Fig. 6. Furthermore, we model the influence of the damper, coolant supply unit device and workpiece as additional vertical linear elastic supports of the corresponding mass points of the boring bar model. This is exemplarily illustrated in Fig. 6 by the vertical spring with stiffness k_{damper}.
Adopting the x-coordinates of the mass points as generalized coordinates and assuming only small deflections we can write the homogeneous equations of motion of the system as a sum of inertial and spring forces:

$$[M]\{\ddot{x}\} + [K]\{x\} = \{0\} \tag{1}$$

with the mass-matrix $[M]_{n\times n} = m \cdot I_{n\times n}$ and the stiffness-matrix

$$[K]_{n\times n} = \frac{k}{l^2}\begin{bmatrix} 6 & -4 & 1 & 0 & \cdots & \cdots & 0 \\ -4 & 6 & -4 & 1 & \ddots & & \vdots \\ 1 & -4 & 6 & \ddots & \ddots & \ddots & \vdots \\ 0 & 1 & \ddots & \ddots & -4 & 1 & 0 \\ \vdots & \ddots & \ddots & -4 & 6 & -4 & 1 \\ \vdots & & \ddots & 1 & -4 & 5 & -2 \\ \vdots 0 & \cdots & \cdots & 0 & 1 & -2 & 1 \end{bmatrix}$$

$$+k_{damper}\{e_d\}\{e_d\}' + k_{seal}\{e_s\}\{e_s\}' + k_{tool}\{e_n\}\{e_n\}'. \tag{2}$$

The equations of motion can be determined by calculating the terms of the kinetic and potential energy of the model of equation 1 in applying Lagrange equations. By doing so the form of matrix 2 is directly obtained. The stiffness k therein can be calculated as a function of the number of degrees of freedom n of the model as it is shown below. The indices d and s represent the position of the mass-points counted from the left, lying within the ranges of contact between the boring bar and the damper or the seal within the coolant supply unit device, respectively. The variables k_{damper} and k_{seal} represent the stiffness of the corresponding support springs. The support of the boring bar through contact with the workpiece is modelled via stiffness k_{tool} acting upon the rightmost mass point of the bar. We assume these parameters to be constant over the complete drilling process.
The stiffness k of the spiral springs can be calculated via comparison with the deflection of an Euler-Bernoulli-Beam [3]. An Euler-Bernoulli-Beam under single-sided rigid restraint conditions and loaded with a transverse force F acting upon its free end shows a maximum deflection of

$$x_{EB,max} = \frac{Fl^3}{3E_{EB}I_{EB}} \tag{3}$$

in the same location and in direction of the force. l,E_{EB} and I_{EB} denote the length of the beam, it's Young's modulus and area moment of inertia. From this, by the definition of stiffness as $F = k_{EB}x_{EB}$ a static stiffness value of

$$k_{EB} = \frac{3E_{EB}I_{EB}}{l^3}. \tag{4}$$

can be calculated. For our discrete model with n degrees of freedom, the same load case results in the deflection x_n calculated as

$$x_n = \frac{F}{k}\, l^2 \sum_{i=1}^{n} i^2. \tag{5}$$

By demanding equivalent static properties from the discrete model, by replacing $x_{EB,max}$ of equation 3 by x_n in equation 5 one can calculate the stiffness k of the spiral springs as a function of the chosen number of degrees of freedom n to be

$$\frac{Fl^3}{3E_{EB}I_{EB}} = \frac{F}{k(n)} l^2 \sum_{i=1}^{n} i^2 \tag{6}$$

$$\Leftrightarrow \quad \frac{l^3}{3E_{EB}I_{EB}} = \frac{1}{k(n)} l^2 \sum_{i=1}^{n} i^2 \tag{7}$$

$$\Leftrightarrow \quad k(n) = \frac{3E_{EB}I_{EB}}{l^3} l^2 \sum_{i=1}^{n} i^2 \tag{8}$$

$$\Leftrightarrow \quad k(n) = k_{EB} l^2 \sum_{i=1}^{n} i^2 \tag{9}$$

In contrast to l, m and k the values of the parameters k_{damper}, k_{seal} and k_{tool} are not known.

Now determining the n BEFs ω_r and corresponding bending eigenmodes (BEMs) $\{\Psi\}_r$, $r = 1, \ldots, n$, of the system means solving the following eigenvalue-problem:

$$\left([K] - \omega_r^2 [M]\right) \{\Psi\}_r e^{i\omega_r t} = \{0\}. \tag{10}$$

for which the only non-trivial solutions satisfy

$$det \left|[K] - \omega_r^2 [M]\right| = 0. \tag{11}$$

The solution can be expressed in two $n \times n$ - matrices $[\omega_r^2]$ and $[\Psi]$. $[\omega_r^2]$ is a diagonal matrix with ω_r^2 being the r^{th} eigenvalue, or squared natural frequency of the system and the eigenvector $\{\Psi\}_r$, the r^{th} column of $[\Psi]$, being the description of the corresponding mode shape. One can determine

$$[m_r] = [\Psi]^T [M] [\Psi] \tag{12}$$

and

$$[k_r] = [\Psi]^T [K] [\Psi]. \tag{13}$$

$[m_r]$ and $[k_r]$ are also diagonal matrices and m_r, k_r are referred to as *modal mass* and *modal stiffness* of mode r.

A BEM is the shape with which the bar oscillates with the corresponding BEF. Each BEM is represented by the vector $\{\Psi\}_r$ containing the deviations from the baseline in x-direction for each segment end (compare Fig. 6).

Now the time-variation of the BEMs and BEFs becomes clear when looking at what happens during the drilling process. The boring bar is fixed to a drive unit on the left side and when the process starts the workpiece is rotated and drive unit together with tool/boring bar assembly and damper are moved towards the workpiece. While the damper always stays in the same position d relative to the boring bar, the seal on the coolant supply device stays at a fixed distance from the workpiece and therefore moves with

a constant speed relative to the bar. So s decreases and the stiffness matrix $[K]$ changes. Note that even though workpiece and boring bar move relative to each other, k_{tool} is always added to the nth element of the "base" matrix in the first row of the definition of Eq. 2. This is because the workpiece always affects the end of the bar.
In order to be more realistic, additional viscous damping $[C]$ is included in the model [1]. The equation of motion then changes to

$$[M]\{\ddot{x}\} + [C]\{\dot{x}\} + [K]\{x\} = \{0\}.$$

To reduce the number of parameters, often a special case called *general proportional damping* is used (see Ewins, pp. 64-66). The matrix $[C]$ then is assumed to be a linear combination of

$$[C] = \beta[K] + \gamma[M].$$

In this case the mode shape vectors $\{\Psi\}_r$ stay the same as in the undamped model. The system's eigenfrequencies change to

$$\omega_r' = \omega_r\sqrt{1-\zeta_r^2} \tag{14}$$

with $\zeta_r = \beta\omega_r/2 + \gamma/(2\omega_r)$ being the viscous damping ratio of the r^{th} mode. As mentioned above the stiffness parameters k_{damper}, k_{seal} and k_{tool} and the parameters β and γ to construct the damping matrix are not known. In early experiments it turned out that the higher the value chosen for k_{tool} – i.e. if the end of the bar is almost prevented from moving – the better is the model fit. So k_{tool} from now on is fixed to a high value ($10^{17}\,\mathrm{N/m}$) and the remaining free parameters are k_{damper} and k_{seal}, β and γ. An additional parameter $k_{damper-end}$ is included in the model to allow for non constant spring stiffness over the range of contact between the damper and the boring bar. Its stiffness-values are given by k_{damper} and $k_{damper-end}$ at both ends and the values between are linearly interpolated.
We use the model at given parameters to calculate the *frequency response function* [FRF] $\alpha_{jk}(\omega)$. This function allows to calculate the response of system at point k to excitation at point j at a given frequency ω. Of course, at rest the boring bar does not show any movement. If the bar is excited by some(sinusoidal) force of frequency ω at any position k the resulting deflection of the bar at each point k can be calculated by multiplying the excitation-amplitude with the frequency response function $\alpha_{jk,t}(\omega)$, where

the additional index t here only denotes that the model changes during the process time t due to different positions of the damper and the oil supply along the boring bar. In our case of general proportional damping, this function is given by (Ewins, 2000, pp.62-65):

$$\alpha_{jk}(\omega, t) = \omega^2 \sum_{r=1}^{n} \frac{\Psi_{jr,t}\Psi_{kr,t}}{k_{r,t} - \omega^2 m_r + i\omega c_{r,t}} \tag{15}$$

with the diagonal modal damping matrix $[c_{r,t}] = \beta[k_r] + \gamma[m_r]$ and $\Psi_{jr,t}$ being the element of $[\Psi_t]$ of row j and coloumn r.
Figure 7 illustrates the system's calculated FRF (for fitted parameter values) at some fixed moment during the process as well as a slice of the periodogram at the same time.

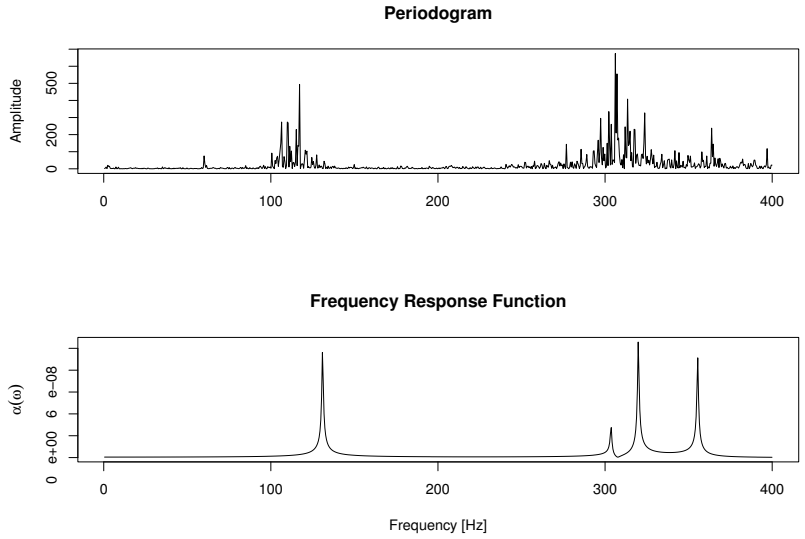

Figure 7: Slice of the observed periodogram and the calculated FRF for fitted model parameters at the same time.

The function $\alpha_{jk}(\omega)$ is used to estimate the five missing parameters to build the model. How this can be done is explained in the following section.

4 Criterion

For a given set of parameters one can calculate the response to excitation in any specific frequency. The idea consists in fitting the calculated FRF to the observed periodogram and thus to find the model parameters that best fit the data. We assume that the boring bar is mainly excited through the cutting process at the tools point of contact with the workpiece and that all other sources of excitation can be neglected. The acceleration sensor is positioned at position $k = 150\,cm$ between the damper and the coolant supply device. The FRF is modelled for excitation at the position $j = 334\,cm$ at the boring bar's end.

Apart from the unknown model parameters unfortunately also nothing is known about the spectrogram of the excitation of the system at a given time. The most practical case for analysis would be a white noise-excitation because of its flat spectrum. The observed data then would directly represent the shape of the FRF. Ibrahim et al. [4] therefore propose to use a *pseudo-FRF* $\alpha^*(\omega)$ that transforms white noise into the true but unknown excitation. The response of the system at frequency ω is then the product $\alpha^*(\omega)\alpha_{jk}(\omega)$ of both filters. The poles of both frequency response functions are retained in the product.

Therefore, a peak in the observed periodogram may either be a result of the pseudo-response of the excitation to white noise or a result of the frequency response of the system. We are therefore searching for a model that optimally reflects the system's response in the observed data. We require all strongly represented frequencies in the (fitted) FRF of the model also to be recognizable in the observed data. Hence, the criterion to find optimal model parameters is defined in the following way:

$$criterion(k_{seal}, k_{damper}, k_{damper-end}, \beta, \gamma) = \int_t \int_\omega \frac{A(\omega,t)|\alpha_{334,150}(\omega,t)|}{\int_{\omega^*} |\alpha_{334,150}(\omega^*,t)|\, d\omega^*}\, d\omega\, dt, \tag{16}$$

where $A(\omega, t)$ is the observed amplitude of frequency ω at time t in the periodogram and $\alpha_{334,150}(\omega, t)$ is the frequency response function at time t. Here only its absolute value of the FRF is of interest since we are only investigating the amplitudes of the observed periodogram and are not interested in the phase of the signal (relative to the unknown excitation).

This criterion can be interpreted as weighting the observed periodogram, according to the estimated system's frequency response, temporarily nor-

malized over all frequencies ω at a given time t and averaged over the whole time course of the process. This criterion is supposed to be large for a good model where all strongly represented frequencies in the (fitted) FRF are also weighted strongly by their observed value in the periodogram data. This criterion should therefore be maximized.

5 Results

The criterion as described above is used to indicate a good fit of the model. Parameter fitting is done by the search-based method of Nelder and Mead [5]. To avoid local minima at parameters still badly fitting the data as they are often found by such optimization algorithms, a grid search 'by hand' was performed to find the magnitude of parameter combinations yielding good results. A combination of these parameters is then used as initialization for implementation of the optimization algorithm. The parameter seed was set as follows: $k_{seal} = 1 \cdot 10^7\, N/m$, $k_{damper} = 1 \cdot 10^7\, N/m$, $k_{damper-end} = 1 \cdot k_{damper}$, $\beta = 5 \cdot 10^{-7}\, s^{-1}$ and $\gamma = 5\, s^{-1}$.
The measured acceleration of the boring bar (log scaled amplitudes) is given in figure 8.

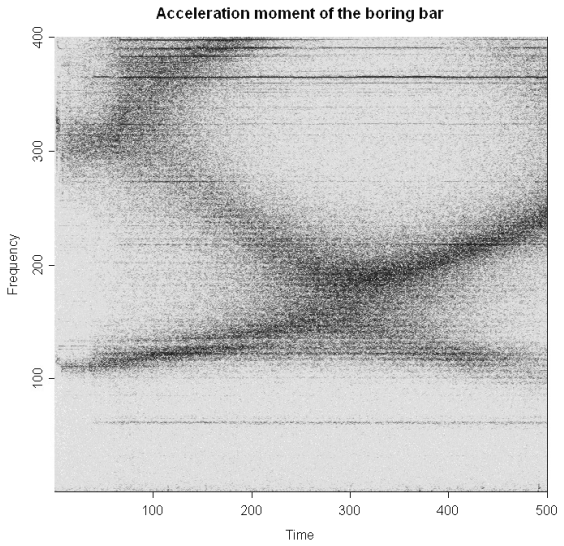

Figure 8: Observed periodogram data.

Optimization with the Nelder/Mead-algorithm in the example returns parameters $k_{seal} = 1.1 \cdot 10^7\, N/m$, $k_{damper} = 1 \cdot 10^7\, N/m$, $k_{damper-end} = 3.64 \cdot k_{damper}$, $\beta = 2.16 \cdot 10^{-11}\, s^{-1}$ and $\gamma = 4.97\, s^{-1}$.
The left figure in figure 9 shows the (log scaled) weighted periodogram by the estimated system's frequency response as they are used for fitting the parameters. One can see a few strongly weighted frequencies at any depth. This indicates that the estimated frequency responses fits the observed periodogram quite well which is not the case on the right hand side. There, the weighted periodogram of the criterion for a still reasonable but worsely fitting model is shown.

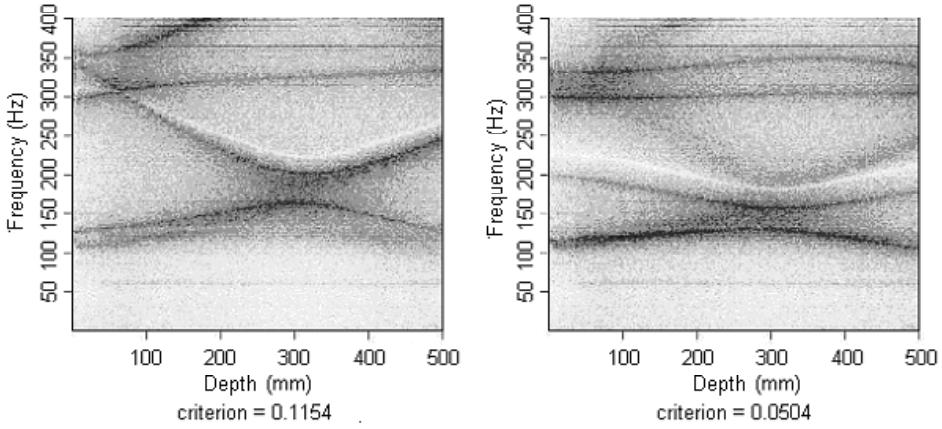

Figure 9: Weighted periodograms (as they are used for fitting the parameters) of the optimal solution (left) and a 'bad fit' (right) at stiffnesses of 20% of the model on the left hand side.

6 Outlook

To investigate the validity of the model introduced here statistically, computer simulations will be performed. There, for given sets of parameters the resulting spectrograms will be calculated. Thereupon, these spectrograms are used to generate stochastic processes. After adding noise and estimating the parameters based on the obtained noisy processes the validation will be done by comparing the resulting fitted eigenfrequencies to the real ones with respect to bias.

The model can be a basis for both offline and online process control. Offline methods concern choices of parameter settings for which intersections of the corresponding eigenfrequencies and multiples of the rotational frequency will not occur. This can also be achieved by a priorily planned variation of the rotational speed.
Online methods concern the supervision of the predicted eigenfrequency courses. Therefore each reasonable variable parameter e.g. the unknown stiffnesses should be controlled with respect to given *specification limit bands*. These limits should be chosen so that exceeding them indicates an oncoming intersection of a bending eigenfrequency with a multiple of the rotational frequency. Control charts will be developed to supervise the parameters during the process. These control charts will produce alarms whenever their values exceed the specification limit with a high probability according to some prespecified probability level.
Intervention strategies like variations of the rotational frequency can directly be derived from the model and will be tested.
The development of control charts will also be supported by computer simulations. There, different parameter distributions and trends will be investigated as well as different error types.

7 Summary

Through the presented model we established a connection between measured data and the mechanics of the BTA system. As can be seen in the previous section, the dynamics of the system's calculated eigenfrequencies can be found quite well in observed periodogram data. This indicates that our mechanical model realistically represents the behavior of the boring bar during the process.
Goals of future work now have to include the reduction of calculation-time. Furthermore the error distribution of the estimation has to be investigated. Having such knowledge, a strong tool is developed to prevent crossing of one of the system's eigenfrequencies with a multiple of the rotation frequency and thereby to prevent spiralling.

Acknowledgment

This work has been supported by the Collaborative Research Center 'Reduction of Complexity in Multivariate Data Structures' (SFB 475) of the German Research Foundation (DFG).

References

[1] EWINS, D. (2000): *Modal testing: theory, practice and application.*, 2. ed., Research studies press, Baldock.

[2] GESSESSE, Y.B., LATINOVIC, V.N., and OSMAN, M.O.M. (1994): On the problem of spiralling in BTA deep-hole machining. *Transaction of the ASME, Journal of Engineering for Industry, 116*, 161–165.

[3] GROSS, D., HAUGER, W., SCHNELL, W. and SCHROEDER, J. (2005): *Technische Mechanik Band 2: Elastostatik*, 8. ed., Springer, Berlin.

[4] IBRAHIM, S., BRINCKER, R. and ASMUSSEN, J. (1997): Modal parameter identification from responses of general unknown input, *SPIE Proceedings 2968 of the 14th International Modal Analysis Conference*, 446-452

[5] NELDER, J.A. and MEAD, R. (1965): A Simplex Method for Functional Minimization. *Computer Journal, 7:308–313.*

[6] RAABE, N., THEIS, W., and WEBBER, O. (2004): Spiralling in BTA Deep-Hole Drilling - How to model varying frequencies. *Conference CD of the Fourth Annual Meeting of ENBIS 2004*, Copenhagen.

[7] RAABE, N., THEIS, W., WEBBER, O., WEIHS, C. (2005): Spiralling in BTA deep-hole drilling – Models of varying frequencies, *In: Spiropolou, Gaul: Proceedings of the 29th GfKl annual Conference in Magdeburg*, (accepted paper).

[8] STOCKERT, R. (1978); *Beitrag zu optimalen Auslegung von Tiefbohrwerkzeugen*, Dissertation, Fachbereich Maschinenbau, Universität Dortmund

[9] THEIS, W. (2004): *Modelling Varying Amplitudes*, Dissertation, Fachbereich Statistik, Universität Dortmund, http://eldorado.uni-dortmund.de:8080/FB5/ls7/forschung/2004/Theis

[10] VDI (1974): VDI-Richtlinie 3210: Tiefbohrverfahren. *VDI Düsseldorf.*